Getting the Mass of the First Construction Climber Under 900 Kg

Larry Bartoszek, P.E.[1]
Bartoszek Engineering, Aurora, IL, 60506

In 2004 I presented a conceptual design for the drive system of the first construction climber as outlined in Edwards' and Westling's book on the Space Elevator. My first design used non-spaceworthy components as placeholders to see how close to the mass budget I could come. The first design was approximately a factor of three too heavy.

The current design uses finite element analysis to minimize the mass of structural members to better fit into the mass budget.

Some of the original concerns about the design are still problematic. Axial gap motors in the necessary power range of 20kW and up have not been widely developed for Earth use yet because of recent economic and political conditions.

This paper will describe the engineering effort to redesign the first construction climber and discuss some of the challenges to reach final engineering.

I. Introduction

THIS paper builds on the conceptual design of the traction drive of the first construction climber presented by the author at the 2004 International Space Elevator Conference in Washington, D.C.[1] It compiles work done since 2004 to lighten the structure because the initial conceptual design was 2.4 times too heavy to satisfy the mass budget. Recent advances in the understanding of high cycle metal fatigue allow the relaxation of some of the design constraints used in the first conceptual design. The paper also presents a mathematical analysis of the velocity profile of the climber subject to real power constraints and wheel material strength. The math will show that not all of the requirements of the first construction climber can be satisfied simultaneously with currently existing motor technology. The safety factor of the ribbon is also discussed in the context of the acceleration achievable by the climber. Finally, some observations on the climber are presented from a mechanical engineering perspective about the location of the center of mass of the climber and how that could affect the ribbon.

II. Theory of the traction drive of the Space Elevator Climber

The design of the climber starts with the most general requirements. The climber is supported by the ribbon using friction alone. The support from friction comes from squeezing the ribbon between powered rolling elements and the coefficient of friction between the rollers and the ribbon. The design of the traction drive in Edwards' and Westlings' book uses a tread wrapped around wheels similar to a tank's design. It is easy to show mathematically that the tread is not a useful addition to the design and must be eliminated from the conceptual design. My original conceptual design used pairs of wheels clamped to each other with the ribbon in between.

The parameter that determines how tightly the wheels must squeeze the ribbon is the coefficient of friction between the ribbon and wheels. If the ribbon is too slippery it may not be possible to squeeze it hard enough to develop the traction needed to lift the climber.

The theory starts with a free body diagram of a single wheel pair pushed against the ribbon as shown in Figure 1. The wheel on the opposite side of the ribbon is not shown, but it provides the symmetric reaction force to the compression force F. (The wheels are clamped to each other around the ribbon through the structure of the climber.) The free body diagram neglects the losses from bearing friction and rolling friction. This model assumes that the entire weight of the climber is supported by a single wheel pair. If the climber is supported by more than one wheel pair, the weight is assumed to be distributed equally between all the wheel pairs, so the m_c term would be divided by the number of wheel pairs. This is similar in concept to the addition of locomotives to pull ever longer trains.

---

[1] Owner, 818 W. Downer Place, Aurora, IL 60506.

An equation of motion for the climber can be written by summing the moments around the point of contact between the wheel and ribbon.

$$\sum M = T - \frac{m_c \ddot{r} R}{2} - \frac{m_c g(r) R}{2} - J\alpha = 0 \tag{1}$$

Where:
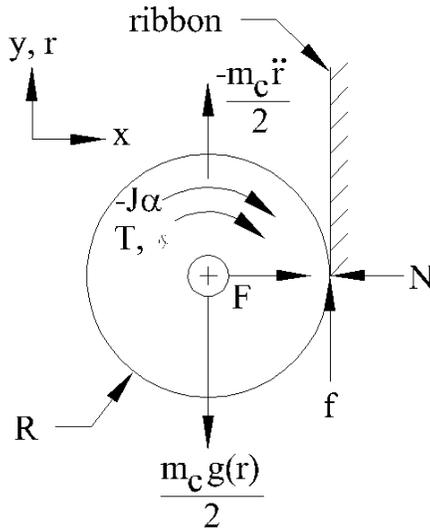
Figure 1. Free body diagram of a wheel pressed against the space elevator ribbon. The force F is balanced by the reaction force coming from the wheel on the opposite side of the ribbon.

M = moments summed around point of contact between wheel and ribbon

R = radius of the wheel

N = normal force between ribbon and wheel

F = applied force compressing wheel to ribbon

T = applied torque from drive train

m_c = mass of the climber = 900 kg

f = friction force between ribbon and wheel

g(r) = gravitational drag force expressed as a function of r, radius from the center of the Earth

$$g(r) = \frac{M_e \cdot G}{r^2} - r \cdot \omega^2$$

G = Newton's gravitational constant

$$G = 6.67 \cdot 10^{-11} \cdot \frac{m^3}{sec^2 \cdot kg}$$

M_e = mass of the Earth

$$M_e = 5.9788 \cdot 10^{24} \cdot kg$$

ω = angular velocity of the Earth about its axis

$$\omega = 7.2929 \cdot \frac{10^{-5}}{sec}$$

J = rotary mass moment of inertia of wheel, kg-m^2

α = rotational acceleration of wheel, sec^{-2}

$\ddot{r}$ = linear acceleration along ribbon

x, y = Cartesian coordinates, y along ribbon, x perpendicular to face of ribbon

θ = Angle of rotation around the axis of the wheel, radians

The contact is assumed to be rolling and not sliding, so the linear and angular positions, velocities and accelerations are related by the following expressions:

$$r = R\theta,$$

$$\dot{r} = R\dot{\theta} \text{ and}$$

$$\ddot{r} = R\ddot{\theta} = R\alpha$$

Rearranging the terms of equation 1 and making the appropriate substitutions gives an equation for the torque required to accelerate the climber upwards with any given linear acceleration $\ddot{r}$:

$$T = \ddot{r}\left(\frac{J}{R} + \frac{m_c R}{2}\right) + \frac{m_c g(r)R}{2} \tag{2}$$

The left side collection of terms (to the right of the equal sign) are the inertial terms. These give the torque required to accelerate the climber from any given initial velocity to any final velocity. The second expression in the sum can be thought of as the braking torque required to hold the climber on the ribbon at a point and not let it roll down the ribbon. This is one of the conceptual differences between an electric car on earth and the climber on the space elevator. Typically on Earth the car is not required to exert a constant torque just to stand still. This second term is critical in the analysis below with real motor characteristics because it never goes away. In constant velocity analyses, the r-double-dot acceleration term is zero so the the right term is the only one to consider. As the climber rises, the pull of gravity declines with an inverse square relationship, but for thousands of kilometers near Earth, the climber must exert a significant braking torque.

This equation is the reason that an additional track makes no sense in the design of the traction drive. Looking at the free body diagram, it is clear that the friction force can only be applied at the point of contact between the wheels and the ribbon. In between wheel pairs there cannot be a normal force pushing a track against the ribbon. Without a normal force, there is no friction force, so no traction. The sections of the track in between wheel pairs cannot contribute to the traction. The J term is the rotary mass moment of inertia of the drive wheel/tread system. The existence of a track increases J and thereby decreases the acceleration achievable when the torque is fixed at a maximum, while also increasing the mass of the traction drive *and not contributing to traction*.

These mathematical arguments lead me to discard the track from Edward's original design and focus on a traction drive with wheels only.

To design the wheel compression mechanism that provides the force F, we must know the coefficient of friction between the ribbon and the wheel. This number is not known at present and to get anywhere in the conceptual design, a number must be assumed.

The friction model used here is Coulomb dry friction in which the traction does not depend on the area of contact, but only on the normal force and coefficient of friction as given by equation 3:

$$f = \mu N \tag{3}$$

where μ is the coefficient of friction. I chose to use $\mu = 0.1$ as a reasonable guess at the value of the coefficient. Many dry sliding bearing materials show coefficients in the range of 0.01 to 0.1. Coefficients larger than 0.2 are generally used between structural members designed not to slip on each other. A coefficient larger than 1.0 usually means some adherence is in play between the two surfaces.

μ may have different values depending on whether the contact is sliding (kinetic friction) or not sliding (static friction). The case of sliding contact is considered a failure of the climber's traction, so the kinetic coefficient of friction will not be used in this analysis. Climbers must operate in the regime up to the point of impending sliding and no further, so anytime the coefficient of friction appears in an equation, it is understood to be the static coefficient of friction.

By summing the forces in the x and y directions, we can get a relationship between the normal force F, the mass of the climber, and the coefficient of friction.

$$\sum F_y = f - \frac{m_c g(r)}{2} = 0 \tag{4}$$

$$\sum F_x = F - N = 0 \tag{5}$$

Rearranging (4) gives

$$f = \frac{m_c g(r)}{2} \tag{6}$$

The traction force between the ribbon and the wheel is equal to half the weight of the climber applied to that wheel. (The wheel on the opposite side provides the other half of the friction force needed to support the climber.) Rearranging (5) gives F = N, the normal force coming from the second wheel in the wheel pair (through the ribbon) is balanced by the applied force on the first wheel.

Equation (6) describes the condition in which the weight of the climber is balanced by the friction force, but the friction force required is less than that calculated by equation (3). The condition of *impending sliding* is required to allow equation (3) to be used with equation (6). Substituting F for N in (3) gives f = μF which gives

$$F(\mu) = \frac{m_c g(r)}{2\mu} \tag{7}$$
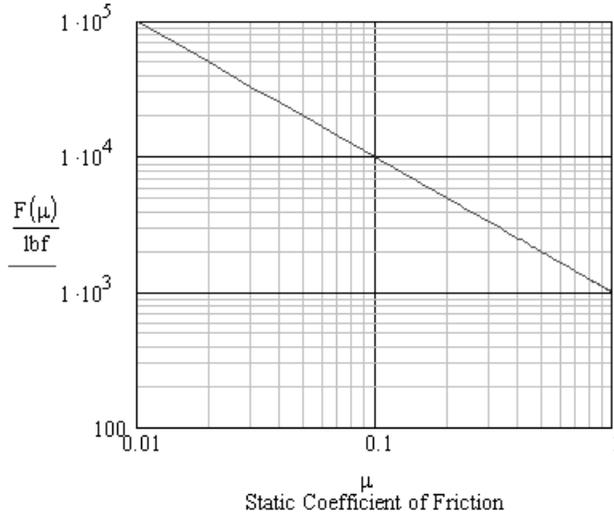
Figure 2. Graph of the compressive force required to squeeze the ribbon as a function of the coefficient of friction between the wheels and ribbon for the 900 kg climber.

The graph in Figure 2 shows that the force required to squeeze the drive system around the ribbon is almost 10,000 lbs (5 tons) if the coefficient of friction is 0.1.

It is easy to see that if the coefficient of friction is too low, the ribbon will become unclimbable.

Also, since the coefficient of friction determines the squeezing force F of the compression mechanism, and this force F has to be absorbed as tension and compression in the structure of the climber, the coefficient of friction determines the stress state of all of the structural elements of the traction drive.

As an aside, the same equation holds for the 20 tonne commercial climber. For those, the clamping force required is 980,000 N or 220,304 lbf (110.2 tons). If there are three wheel pairs on a commercial climber, each wheel pair is compressed together with a force of 36.7 tons. If those compression mechanisms use two screw jacks as shown in the 2004 design, each one has a load capacity of 20 tons.

Given the previous equations, we are now in a position to analyze the power and torque requirements of the motors on the climber for different assumptions of velocity profile of the climber.

Edwards and Westling assumed a velocity for the climber of around 200 km/hr and a total motor power for the first climber of 100 kW. Assuming that the climber climbs with constant velocity (we will ignore the acceleration of the climber for now,) and knowing the torque required to support the climber, the power of the motors is calculated from:

$$P_c(r) := m_c \cdot a_c(r) \cdot v_c \tag{8}$$

where

$P_c(r)$ = Power required to lift the climber at constant velocity

m_c = mass of the climber = 900 kg

$a_c(r)$ = g(r) (shown above), the gravitational drag corrected for altitude and the rotation of the Earth

v_c = velocity of the climber up the ribbon = 200 km/hr
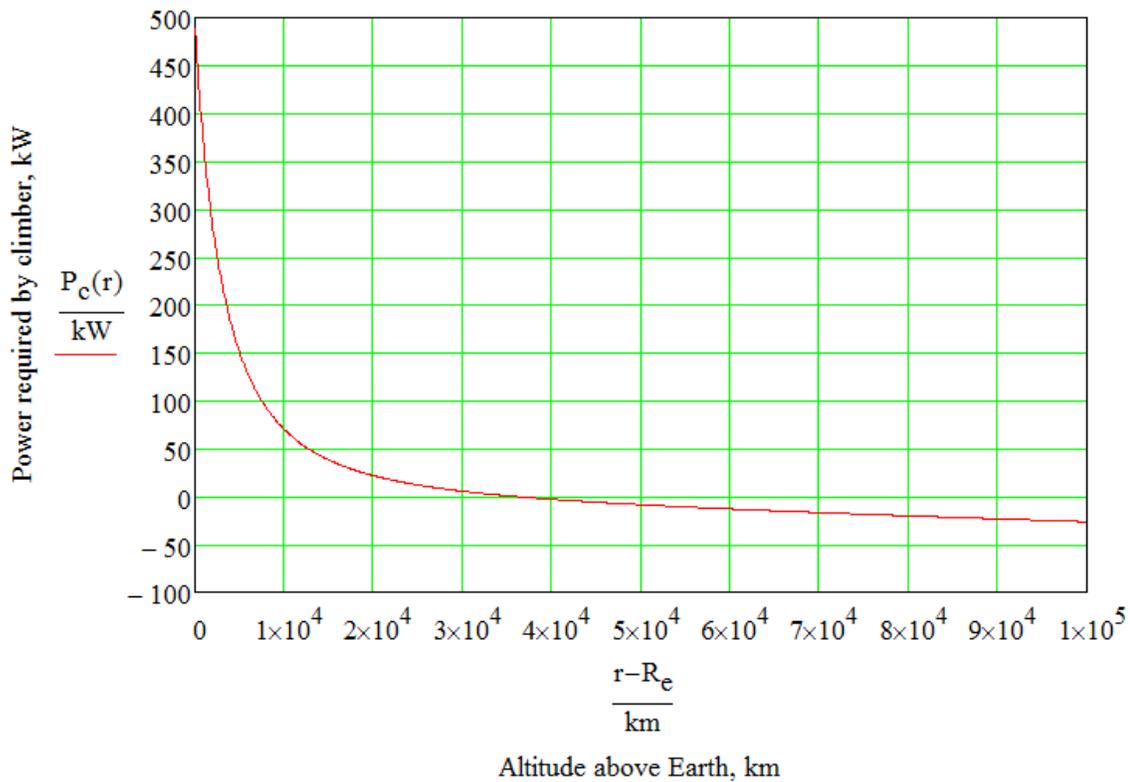
Figure 3. Graph of Power (kW) vs Altitude up the ribbon (km) for the case of a 900 kg climber moving at 200 km/hr constant speed. Geosynchronous altitude is 3.58E4 km up the ribbon and that is where the climber changes from needing power to climb to needing to dissipate power to stop at the end of the ribbon. The graph shows that near the surface of the Earth the power is required to be 488 kW for constant velocity climbing.

The conclusion to reach from the graph is that the assumptions in the book do not work together. The climber requires more than 100 kW to climb at 200 km/hr near the Earth's surface. The power requirement does not drop below 100 kW until an altitude of 7,500 km (4,660 miles) above the surface of the Earth. (For comparison, the altitude of the International Space Station is 370 km (230 miles) up. The Space Shuttle's maximum altitude was 960 km (600 miles).)

If the climber is limited in power at the lower altitudes, the impact is on the travel time. The climber will take much longer to get to the end of the ribbon than the simple constant velocity calculation shows. (100,000 km at 200 km/hr is covered in 20.83 days.)

Another assumption in the book (page 50) is that the climber motors must operate at constant power/variable speed because the laser beaming system delivers constant power. Figure 3 makes it clear that at constant velocity the condition of constant power is not met at all. Even if the beam is delivering a constant power of 100 kW all the way up the ribbon, (which it can't do because the beam will spread with altitude,) constant power isn't needed over the whole trip up the ribbon. Past geosynchronous orbit (GEO) the climber has to dissipate power to be able to stop. As shown in section IV on the wheel analysis below, the mechanism of the climber cannot handle arbitrarily high rotational velocities of its components.

To see the absurdity implied in the constant power assumption all we have to do is rearrange Equation 8 for the case of variable velocity/constant power fixed at 100 kW.

$$v_c(r) := \frac{P}{m_c \cdot a_c(r)} \tag{9}$$

Where P = 100 kW and the velocity is now a variable. The graph of the theoretical velocity is shown in Figure 4. The conclusion from this graph is that as the force of gravity declines with altitude, the climber can go faster and

International Space Elevator Consortium

faster with the constant power, ultimately reaching tens of thousands of kilometers per hour. No climber's wheel rotation mechanism can handle such large dynamic stresses.
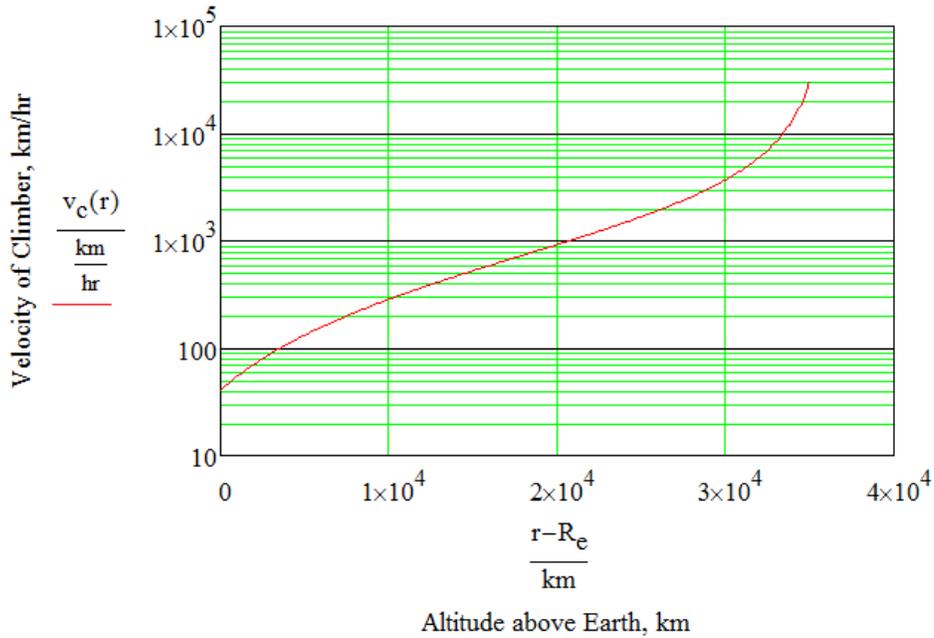
Figure 4. Graph of Climber velocity (km/hr) as a function of Altitude up the ribbon (km). This graph has to be truncated because as the climber approaches GEO the drag force from gravity goes to zero and the velocity goes to infinity.
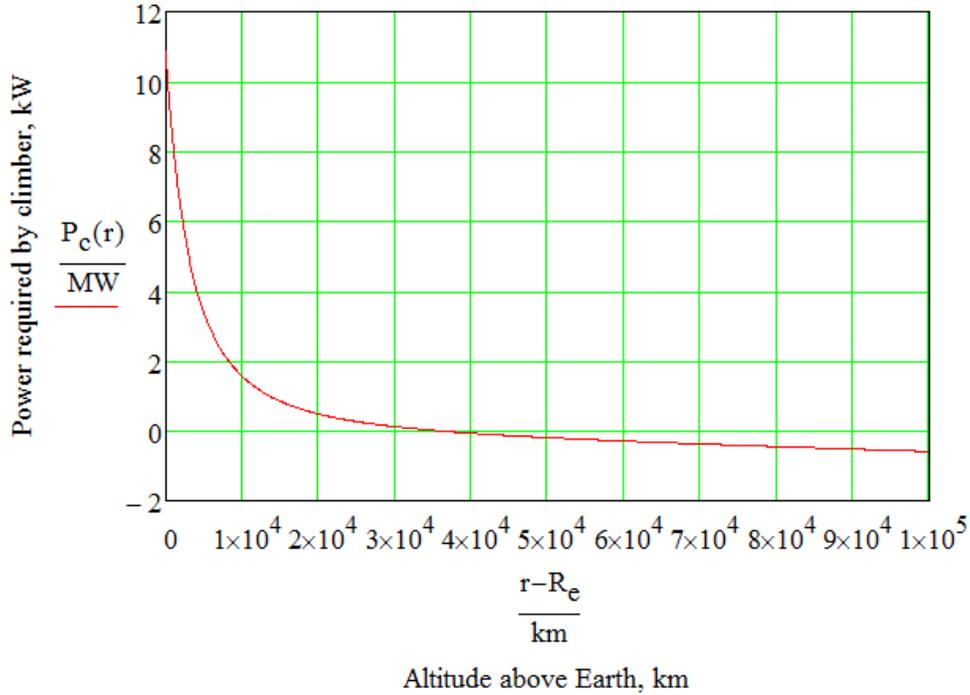
Figure 5. Graph of the power requirement (MW) of the 20 tonne commercial climber as a function of altitude up the ribbon climbing at a constant 200 km/hr. Note that the Y axis is now measured in megawatts. The climber needs almost 11 MW near the surface of the Earth.

International Space Elevator Consortium

This theoretical analysis used no characteristics from a real motor. The analysis becomes even more interesting when the motor characteristics of an actual axial gap motor are folded in as shown below.

As an aside, it is interesting to note the power consumption of the 20 tonne climber. This is shown in Figure 5. The power requirement of the big commercial climbers is not in the single digit megawatts, it is more than 10 MW.

The power graphs make it clear that the hard work is all being done in the first 10,000 km of travel up the ribbon. As the climber goes above this the force of gravity becomes so much smaller that the climber does not need to squeeze the ribbon as hard to get traction, and it doesn't need that much power to climb at several hundred km/hr.

I think this is a strong argument for the use of solar power satellites to feed the climbers as soon as that is practical. Before this is practical, we may have to use naval nuclear reactors like those on the French *Rubis*-class submarines that have a 48 MW reactor.

Using the theory we can take a look at the conceptual design and its weight problem.

III.   The Mass Budget of the First Construction Climber and the Mass Problem of the 2004 Conceptual Design

A rendering of the 2004 conceptual design is shown in Figure 6. The design of the ribbon climber in this paper assumes the mass distribution from Table 3.2 of "The Space Elevator" by Edwards and Westling[2] as the design goal. (Shown here in Table 1.) One goal of the paper is to determine how the original conceptual design of the drive system can be modified so that this re-design is within the mass budget in the table of less than 233 kg. The number 233 kg comes from adding the masses of the Motors, Track and Rollers, and Structure in the table. (The drive system must be less than this number because the entire structure budget cannot be consumed by the traction drive system alone.)
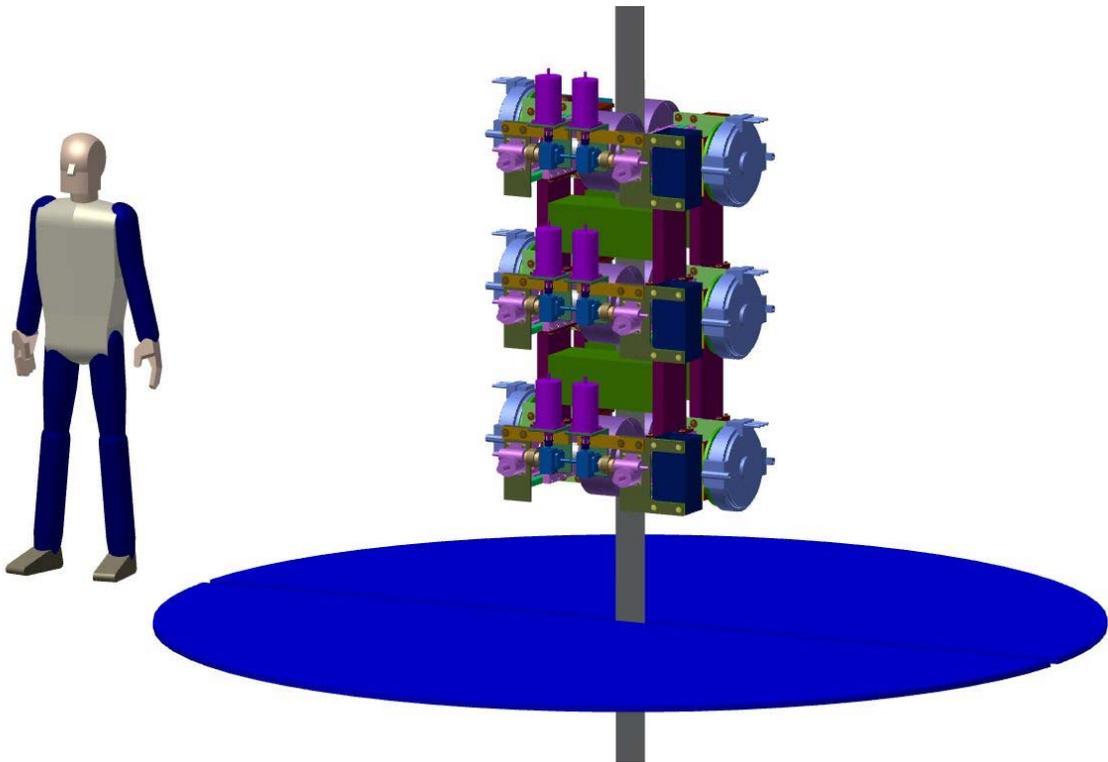
Figure 6. Overall view of the original conceptual design presented in 2004. Design shown is made up of three floating axle drive modules and three fixed axle drive modules. The drive modules are connected to each other by structural weldments. The blue circular segments represent the photovoltaic (PV) planes. No structure is shown connecting the traction drive and the PV plane.

The bottom line of the conceptual design from 2004 is that it could not satisfy the mass budget specified by Edwards and Westling. It was too heavy by a factor of 2.4 with 20 kW motors and 3 with 50 kW motors.

Looking at Table 1, we see that the motors represented almost 56% of the 233 kg budget for the drive train. Table 2 shows that the mass of the motors I found in 2004 made up only 13% of the total mass of the design, and were two thirds of the allowed budget in Table 1. The fact that the motors I used were lighter than the budget for the traction drive meant that the structure was the problem in reducing the mass of the drive. The mass of the conceptual design without the motors was 562.5 kg and the budget for this mass was less than 106 kg. The structure needed to be reduced in mass by a factor of 5.3.

Table 1. Mass distribution of components of the first construction climber

Component	Mass (kg)
Ribbon	520
Attitude Control	18
Command	18
Structure	**64**
Thermal Control	36
Ribbon Splicing	27
Power Control	27
Photovoltaic Arrays (12 m^2, 100 kW)	21
Motors (100 kW)	**127**
Track and Rollers	**42**
TOTAL	900

Also looking at Table 2, the largest contributions to the mass of the traction drive are in the last two lines. Almost 43% of the mass of the conceptual design is in the compression mechanism and structure of the floating wheel modules. Reducing the mass of this part of the traction drive has the biggest effect on the total mass.

The simplest question to ask is, assuming the strengths of different materials are the same so that the structural members are the same size, is there a material less than 1/5 of the density of the aluminum used in the 2004 conceptual design? Looking at Table 3, there are several candidates lighter than aluminum, but only one is lighter than 1/5 of the density of aluminum. Aerographite cannot really be considered similar in strength to aluminum because its ultimate tensile strength is only 23.2 psi. It is a very flexible and weak material. Among the metals, the lightest structural metal is magnesium, but it is 0.66 the density of aluminum, not the needed 0.19. Carbon composite fares slightly better at 0.6 times the density of aluminum and similar strength.

So the simple answer to the simple question is "no". The structure will have to be reduced in cross-section and made of a lighter and stronger material to achieve the weight reduction. Since the original structure was not analyzed for its structural efficiency, it is possible that significant reduction is possible while keeping the material aluminum.

Table 2. Percentage of the total weight of the major components of the conceptual design

Description of climber components:	Climber with 20 kW motors	% of total mass
Mass of 12 self-aligning bearings, kg	16.2	2.51%
Mass of axles, kg	32.1	4.96%
Interface structural material, kg	51.2	7.91%
Mass of 6 wheels, kg	52.7	8.15%
Mass of 6 Schmidt couplings, kg	62.6	9.68%
Mass of structure in 3 fixed wheel modules, kg	70.7	10.94%
Mass of 6 motors, kg	84.0	12.99%
Mass of 3 pairs of compression mechanisms, kg	136.1	21.04%
Mass of structure in 3 floating wheel modules, kg	141.0	21.81%
Total mass of climber traction drive:	646.5	100.00%

Table 3. Various engineering materials in comparison to aluminum.

Material	Density, lb/in^3	Ratio of density to Al
Aerographite	3.07E-04	0.003
Carbon composite	0.058	0.592
Magnesium AZ80A-T5	0.065	0.663
Beryllium	0.067	0.682
Al 6061-T6	0.098	1.000
Titanium, Ti-8Al-1Mo-1V	0.158	1.612
Titanium, Ti-6Al-4V	0.160	1.633
SS 321	0.290	2.959

At the time of the original design one of the design constraints was that the size of the wheels on the climber was determined by limiting the number of revolutions of the wheel to 150 million revolutions to get to the end of a 100,000 km long ribbon. This number of revolutions was thought a reasonable upper limit based on the available fatigue data for many materials. Data beyond 1.5E8 cycles was not commonly available. With the advent of ultrasonic fatigue testing[3], materials can be tested to >1E9 cycles in a few days. This gives a new regime of information about the behavior of cyclically loaded materials.

To achieve the wheel rotation limit of 1.5E8 revolutions, the wheels must be larger than 8.35 inches. Wheels smaller than that will rotate more times to get to the end of the ribbon. In the 2004 conceptual design, the wheel diameter was raised to 12.87 inches based on an analysis of Hertzian contact stress in the wheels.

Given how much the mass of the climber had to be reduced, I decided to examine in detail the design assumption of the number of rotations of the wheel to see if decreasing the diameter of the wheels could cause the rest of the structure around them to be shrunk as well.

Using the new data on high cycle fatigue, assume for the moment that we can allow the wheels to rotate 5×10^8 times or more. The diameter of the wheel comes from the following equation:

$$D = \frac{L}{\pi \cdot n} \tag{10}$$

Where:

D = wheel diameter

L = Length of the ribbon = 100,000 km

n = Allowed number of rotations of wheel = 1.5E8

Plugging these numbers in gives a wheel diameter of 2.5 inches, much smaller than before. If we want to move the climber at 200 km/hr, how fast is this wheel rotating? The answer is 16,709 RPM and this is where the problems start. Axial gap motors in the power range that I have found cannot rotate that fast. The maximum rotation rate I found is 2400 RPM at maximum power.

As the FEA below shows, the effect of the dynamic stress from the wheel rotation is very significant. It is unlikely that we will be able to design a wheel-motor system that can rotate as fast as 10,000 RPM. The dynamic stress quickly exceeds the fatigue limit of the metals in consideration.

If we calculate the speed of the climber with 2.5 inch wheels rotating at only 2400 RPM, the climber will climb at a measly 28.7 km/hr. This is unacceptable for the economics of the space elevator. At 28.7 km/hr, the trip to the end of the ribbon takes 145 days, or 4.8 months.

Figure 7 shows how the number of revolutions of the wheel to get to the end of the ribbon depends on the wheel diameter. At 6.25 inches in diameter, the wheel rotates just over 200 million times to get to the end of the ribbon. The number of revolutions increases dramatically below this diameter requiring very high cycle fatigue testing of all of the wheel and axle materials.

The wheel revolution speed is calculated from the velocity of the climber and the wheel diameter:

$$RPM(D) := \frac{2 \cdot v}{D} \tag{11}$$

Where RPM is the revolutions per minute of the wheel, v is the velocity of the climber and D is the wheel diameter. Figure 8 shows how the wheel revolution speed depends on the wheel diameter for a fixed climber velocity such as 200 km/hr. As we'll see below, any wheel rotation speed of 10,000 RPM or higher is probably not allowed by real materials and wheel size that gives adequate climber speed. Figure 9 shows a graph of the climber velocity as a function of wheel diameter holding the wheel rotation speed fixed at 2400 RPM.
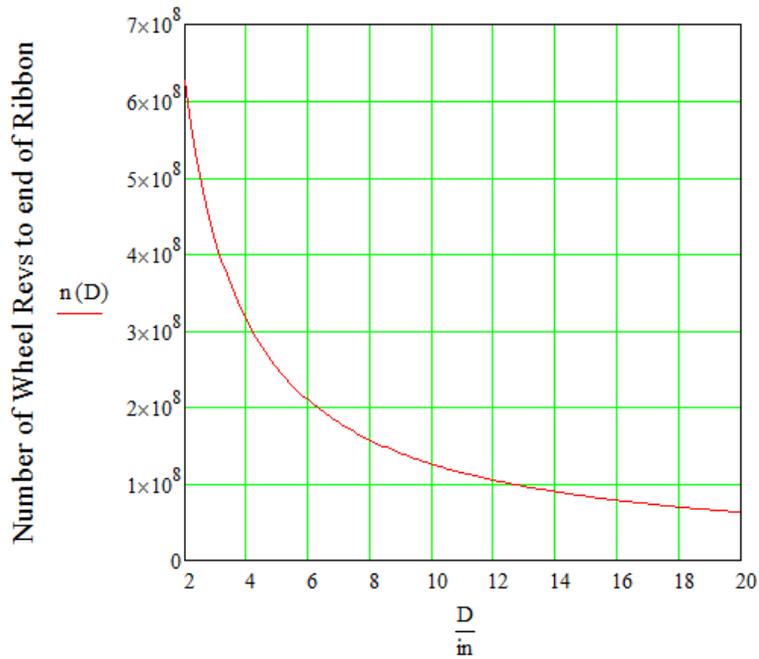
Figure 7. Graph of the Number of Revolutions of the Wheel to get to the end of the Ribbon vs Wheel Diameter. As the wheel decreases in diameter it takes many more revolutions to get to the end of the ribbon. Fatigue strength of every material decreases with increasing cycles of stress. Practical wheels are probably not less than 6 inches in diameter.
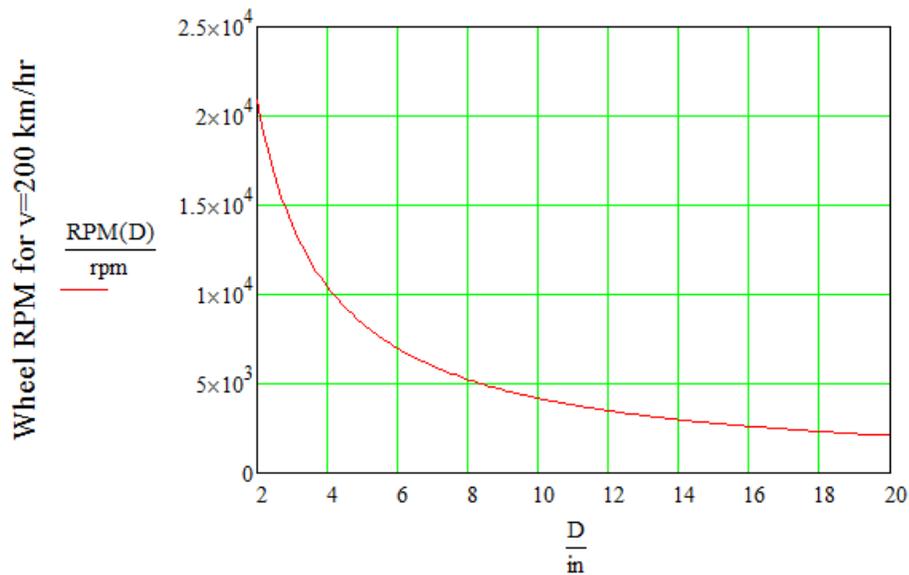
Figure 8. Graph of the Wheel Revolution Speed (RPM) vs Wheel Diameter (inches) at the constant climber velocity of 200 km/hr. As the wheel decreases in diameter, it must rotate faster and faster to keep the climber moving at 200 km/hr. If we have to limit the wheel rotation speed to 10,000 RPM, the wheel must be larger than 4 inches in diameter.

International Space Elevator Consortium
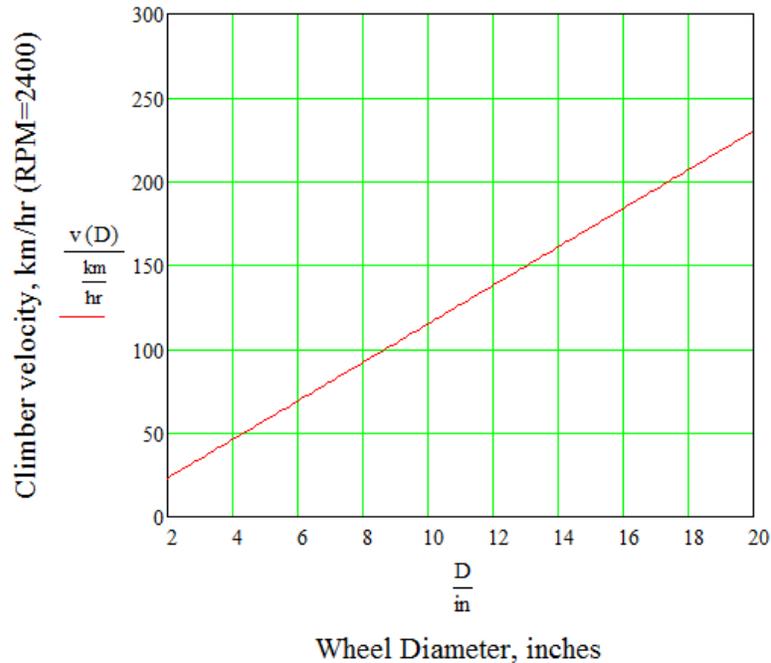
Figure 9. Graph of the Climber velocity as a function of wheel diameter if the wheel revolution speed is fixed at 2400 RPM. We need a climber velocity above 150 km/hr to make the Space Elevator economical to build and operate.

Going back to Equation 2, we see that the braking torque required of the motor is directly proportional to the radius of the wheel. This makes sense. The weight of the climber gets supported by the ribbon through the wheel. The load path for the weight of the climber goes to the bearings on the axle, then through the axle to the hub of the wheel. The larger the wheel, the further away the load is from the ribbon, so the larger the torque required to keep the wheel from rotating.

Motors have a peak torque, or locked rotor torque. This is the amount of torque the motor can apply at zero rotational speed to keep the wheel from turning. From the motor's perspective, it wants the wheel to be small in diameter so that it doesn't need much torq ue to keep the wheel still. Real motors also have a maximum rotation rate (determined by the voltage of the controller) and smaller wheels cause the climber velocity to be lower. Table 4 shows the characteristics of two different axial gap motors from NuGen Mobility, Inc[4]. The mass of these motors is not relevant for the following analysis and they are just used as examples of motors in the right power range.

Table 4.   Characteristics of two axial gap motors from NuGen Mobility, Inc.

Motor Characteristic	MDF240 motor	MDF375 motor
Peak Power, kW	22	100
Cont. Power, kW	12	60
Peak Torque, N-m	110	740
Speed @ Max. Power, RPM	2100	2400
System efficiency	91%	95%

I do not have a complete torque-speed curve for these motors, so a calculation is needed to determine the running torque at maximum speed. The peak torque is fine for a climber that is motionless on the ribbon, but the braking torque term of Equation 2 never goes away. We need to make sure that the torque available from the motor at maximum rotation speed is large enough to keep the climber from rolling backwards down the ribbon. This analysis shows the tight coupling between the motor torque, the wheel size and the speed of the climber up the ribbon.

The climber is designed with a motor on each wheel. There are six wheels in the conceptual design. This means that the total power of the climber is 132 kW if each motor is 22 kW, and 600 kW if each motor is 100 kW. Having

11

the smaller size motor on each wheel is similar to the 100 kW assumption of the first construction climber in Edwards' and Westling's book. (Figure 3 means if we have any hope of running the climber at 200 km/hr near the surface of the Earth, then we need motors closer to the 100 kW rating than the 22 kW rating.)

The continuous torque for the MDF240 motor is calculated by taking the continuous power divided by the rotational speed. This comes out to 54.6 N-m. By rearranging Equation 2 assuming that there are 3 wheel pairs in the climber and the angular acceleration is zero, the size of the wheel comes from:

$$R \leq \frac{6 \cdot T_{cont}}{m_c \cdot g(R_E)} \tag{12}$$

Where $g(R_E)$ is the gravitational acceleration at the surface of the Earth, 9.8 m/s^2. T_{cont} is the continuous torque the motor can deliver. Plugging all the numbers in gives:

$R \leq .037$ m = 1.46 inches, or a diameter of the climber wheel, $D \leq 2.92$ inches. This is much less than the 12.8 inch diameter wheel in the conceptual design. If the rotational speed of the motor is 2100 RPM, then the velocity of the climber up the ribbon with this size wheel is only 29.4 km/hr.

The conclusion from the previous calculation is that the 22kW motor does not have either the power or the torque required to make the climber climb at a reasonable speed. Now let's see how the numbers add up for the larger motor.

The continuous torque for the MDF375 motor comes out to 238.7 N-m. Applying Equation 12 again, $R \leq .162$m = 6.39 inches. The wheel diameter is $D \leq 12.79$ inches. This is very close to the size of the wheel determined for the conceptual design based on Hertzian contact stress criteria.

The maximum velocity of the climber with this size wheel rotating at 2400 RPM is 146.6 km/hr. This is less than the desired 200 km/hr, but not that far off and there may be a way to make up the difference at higher altitudes as shown below.

The next section shows the evolution of the wheel and axle concept and the importance of the dynamic stress.

One conclusion from the calculation with the larger motor is that the wheel does not shrink in diameter significantly if the criteria of climber speed and fatigue stress are to be satisfied. Mass reduction must come from a thorough analysis and redesign of the structure.

IV. Wheel and Axle FEA and Re-design

In 2004 I did not own finite element analysis software. The wheel analysis that was done at the time was done through the favor of a friend. I have since converted the original Mechanical Desktop model of the climber to Autodesk Inventor and now have the finite element package inside Inventor Professional to use. This allows many variations to be tested quickly and for free. The next figures show the stress analysis of the wheel and axle with a series of changes intended to reduce the mass. Since the diameter of the 2004 design was so close to that calculated above, I am using the 2004 model for simplicity.

With a coefficient of friction of 0.1 and three wheel pairs, the force compressing each wheel is 3,333 lbs. Applying this force to the zone of contact of the wheel and constraining the axle at its bearings gives a stress distribution in the 2004 design as shown in Fig. 10.
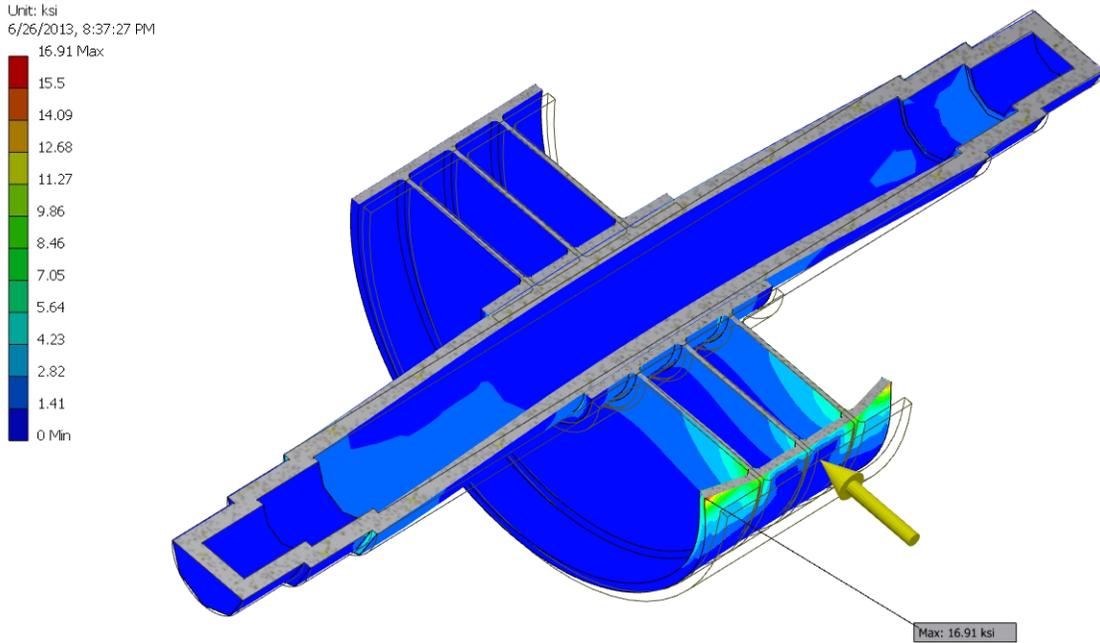
Figure 10. Von Mises stress in the axle and wheel of the 2004 design. This model has no rotational velocity on the wheel. The wall thickness of the aluminum axle is 0.5 inches, which causes the axle stresses to be very low, <3 ksi. The fatigue allowable for Al 6061-T6 is 6.5 ksi at 1.5E8 cycles of reversed bending. (All of the FEA pictures show scaled exaggerated distortion from load.)

The bending of the rim of the wheel is an artifact of the way I am constraining the model.
If I reduce the wall thickness of the shaft to 0.25 inches, the following stress distribution is calculated:
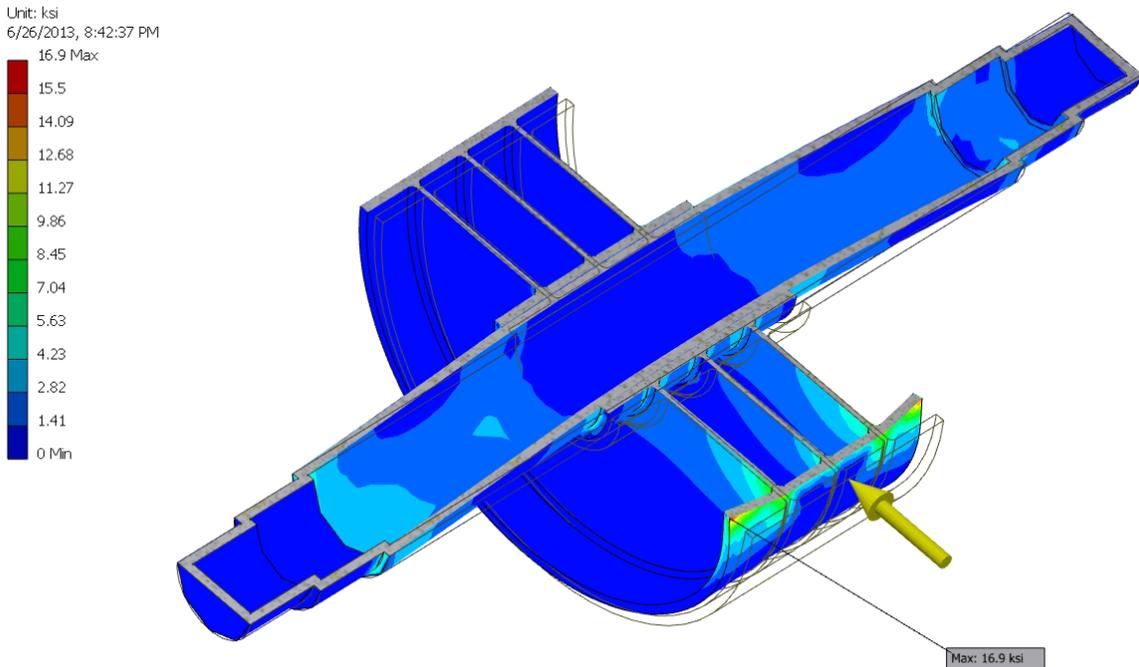
Figure 11. Wall thickness of hollow axle shaft is .25 inches. The maximum stress is still at the edges of the wheel and is an artifact of modeling. Stress in the axle has increased to about 5 ksi maximum near the bearings. Reducing the shaft wall more would violate the stress criterion.

It is clear that most of the web of the wheel is under very low stress. The material used in the model for the wheel is Ti-6Al-4V, a common titanium alloy. Its fatigue strength is much higher than aluminum, 43.5 ksi at 50% confidence at 1E7 cycles of fully reversed bending[5,6]. I do not have data for this material at 1.5E8 cycles, so that could be an issue with using titanium for the wheels. If this titanium alloy survives that many cycles, the stress at 97.5% confidence is certainly much less than 43.5 ksi.

The importance of fatigue to the wheels and axles cannot be overstated. Rolling elements experience fully reversed bending stress which is the most damaging kind of cyclic stress. The rest of the structure that does not roll but carries tensile and compressive stresses can be analysed with static stress models. Fatigue does not play a significant role in the design of the non-rotating structure. Fatigue failure of the rolling elements can lead to chunks of the wheel rim spalling out and damaging the ribbon, or the axle cracking and destroying the entire climber and possibly the ribbon as well. Fatigue is why the allowable stress in the materials of the axle and wheel must be derated so far below their static stress values.

Figure 12 shows the effect of removing material from the web. The concept was to remove material that was at very low stress to improve the efficiency of the material in handling load. To successfully reduce the mass of the climber, every part needs to carry as much load as it can without exceeding fatigue allowable stress for rolling parts and static stress allowables for non-rolling parts.

Figure 13 shows the deflection of the wheel and axle from the compressive load. Axle bending was the reason for selecting self-aligning bearings to support the axle so that the angle made by the bent axle did not overstress the bearings.

Figures 14, 15 and 16 show the effect of dynamic stress on a freely spinning wheel from the rotational speed of the wheel. As discussed below, rotational speed causes dynamic stress that increases very rapidly with speed and ultimately limits how fast wheels and motors can rotate.

Figures 17 and 18 show the combination of the dynamic stress from rotation and the compressive force required to get traction on the ribbon. Figure 17 shows the stress at 2400 RPM and Figure 18 shows the stress at 10,000 RPM.

Shigley[7] shows the radial and tangential stresses in a rotating ring such as the wheel to be:

$$\sigma_t(r) = \rho \cdot \omega^2 \cdot \left(\frac{3+\nu}{8}\right) \cdot \left(r_i^2 + r_o^2 + \frac{r_i^2 \cdot r_o^2}{r^2} - \frac{1+3\cdot\nu}{3+\nu} \cdot r^2\right) \tag{13}$$

$$\sigma_r(r) = \rho \cdot \omega^2 \cdot \left(\frac{3+\nu}{8}\right) \cdot \left(r_i^2 + r_o^2 - \frac{r_i^2 \cdot r_o^2}{r^2} - r^2\right) \tag{14}$$

Where:

$\sigma_t(r)$ = tangential stress in the ring as a function of radius, r

$\sigma_r(r)$ = radial stress in the ring as a function of radius, r

ν = Poisson's ratio for the material of the ring

ρ = density of the ring material

ω = rotational speed of the ring in radians per second

r_i = inner radius of ring

r_o = outer radius of ring

These equations are for a uniform thickness ring whose outside radius is much larger than its thickness. They are illustrative because the stress is a function of the rotational speed squared. In going from 2400 RPM to 10,000 RPM, we are increasing the speed by a factor of 4.2 and the stress by a factor of 17.4. This is born out by the maximum stress numbers in Figures 14 and 15. In going to 40,000 RPM, the speed is increased by a factor of 16.7 and the stress by 277.8. The maximum stress shown in Fig. 16 of 519 ksi exceeds the strength of any metallic material the wheels and axles could be made from. That is why the wheels and motors cannot rotate at an arbitrarily high speed.
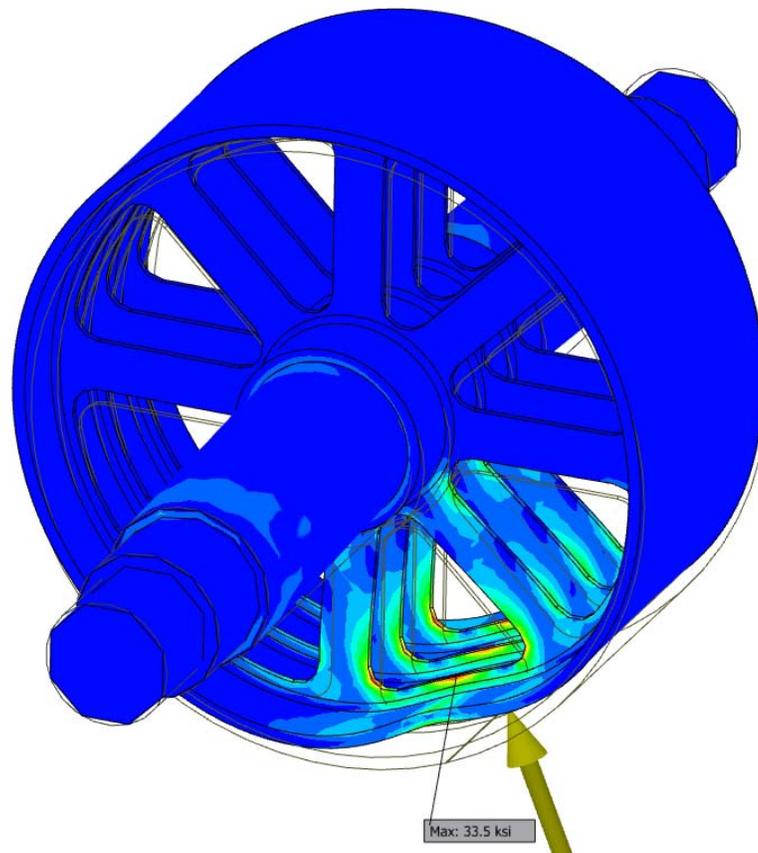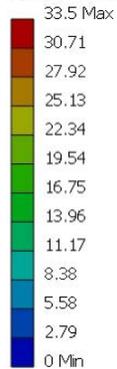
Figure 12.   The maximum stress is shown at the weakest part of the rim of the wheel where material has been removed and peaks at 33.5 ksi, near the 50% confidence fatigue limit of the material. As the wheel rotates, the compression force is alternately applied to the area between the spokes, and then to the spokes. Compression of the spokes needs to be analyzed using buckling stress allowables instead of static stress allowables. Buckling is a geometry dependent failure mode unrelated to the static strength of the material. Buckling can cause failures at very low stresses because the buckling stress allowable is reduced as the spoke becomes more slender.
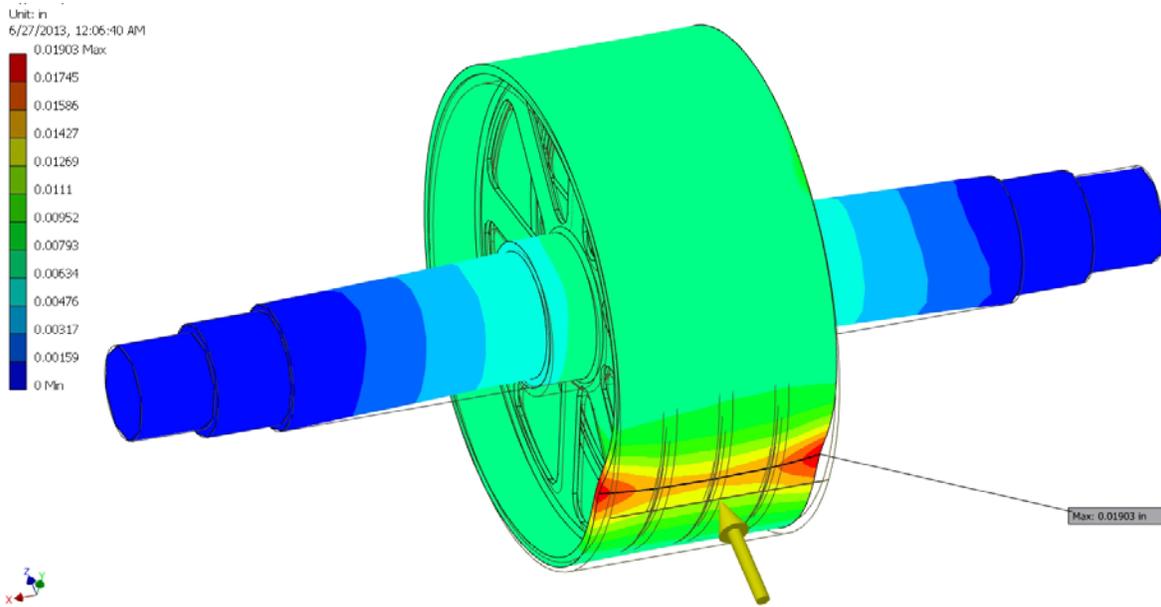
Figure 13. Plot of the deflection of the wheel and axle from the compressive load. The green shade of the wheel shows that the compressive force bends the axles by about 0.008 inches.
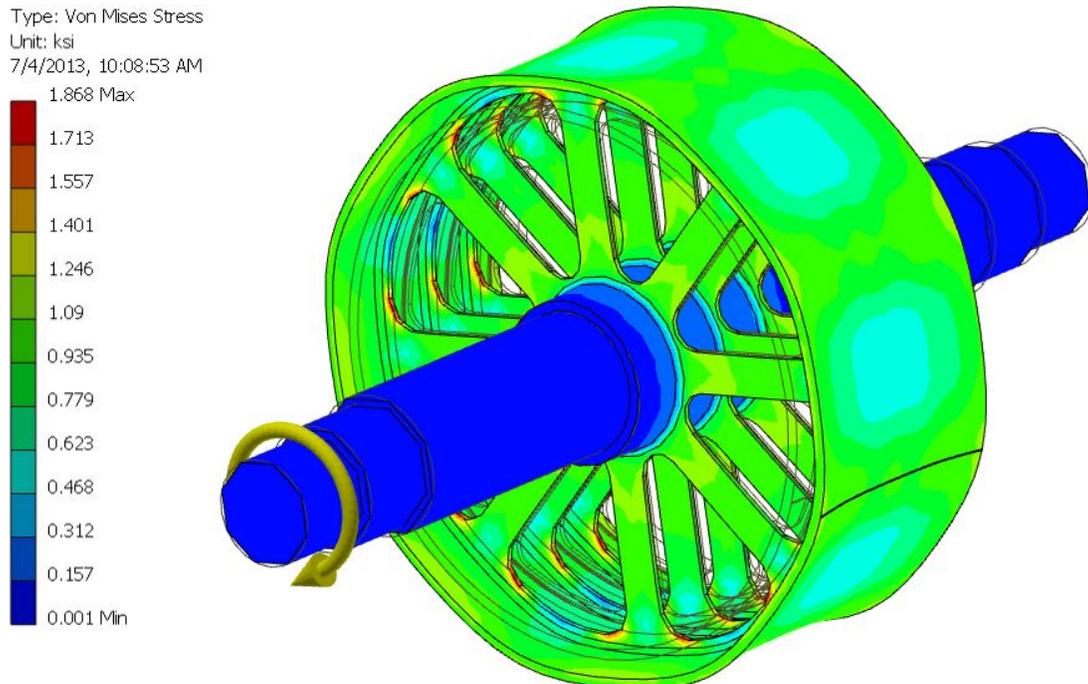
Figure 14. Plot of Von Mises stress for a wheel spinning under no load at 2400 RPM. The maximum dynamic stress is in the fillets of the web cutout. This stress might not be possible to ignore since the material is in fatigue loading. Stress concentrations lead to fatigue crack growth in cyclic loading, where in static stress the material yields locally and the stress can be neglected. The stress is reasonably low at 2400 RPM.

International Space Elevator Consortium
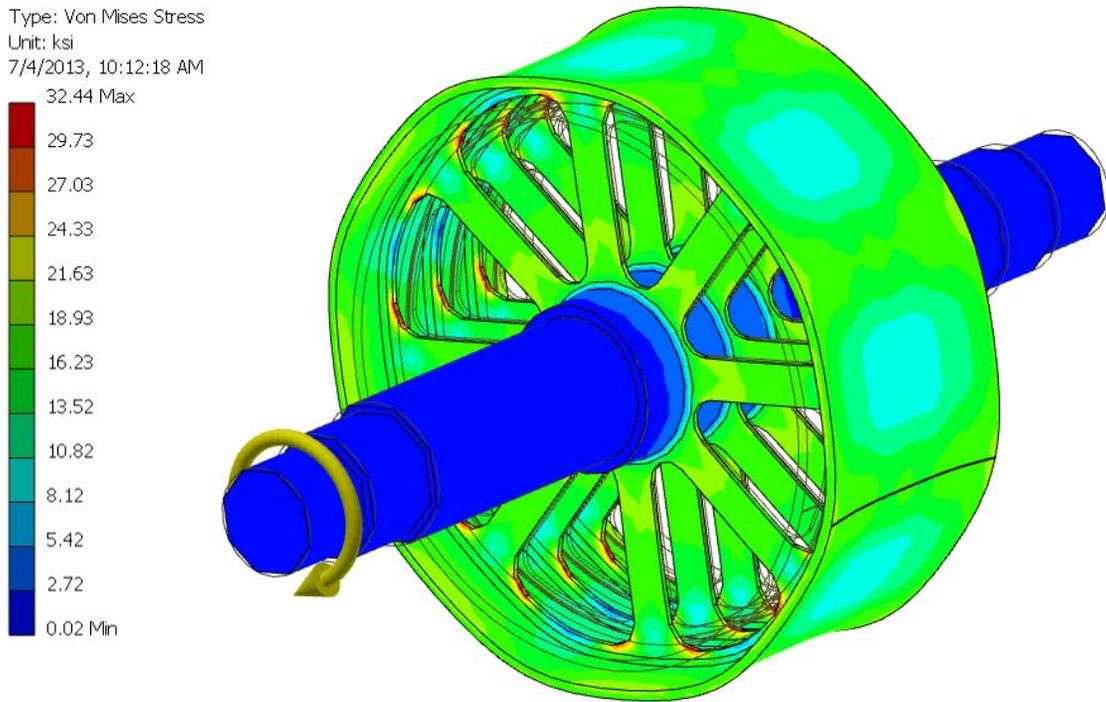
Figure 15. Plot of Von Mises stress for a wheel spinning under no load at 10,000 RPM. The maximum dynamic stress is still in the fillets of the web cutout but is now 32.44 ksi, close to the 50% confidence fatigue allowable for titanium. It is not known if it exceeds the 97.5% confidence level.
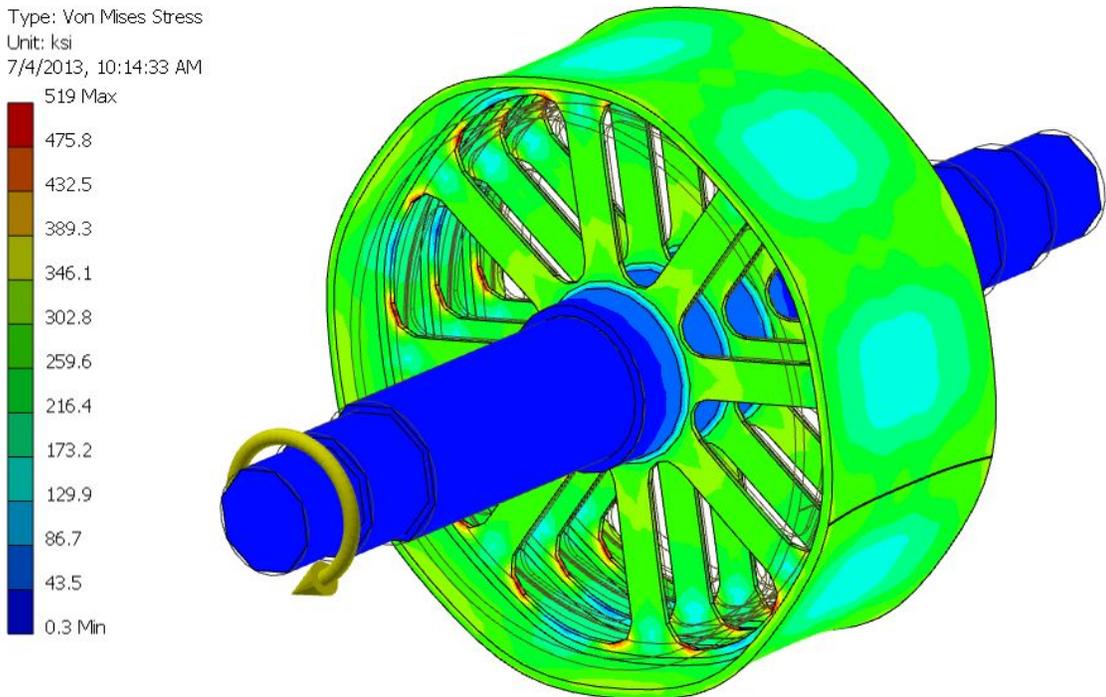
Figure 16. Plot of Von Mises stress for a wheel spinning under no load at 40,000 RPM. The maximum dynamic stress is now 519 ksi. This is higher than any engineering material can withstand.

International Space Elevator Consortium
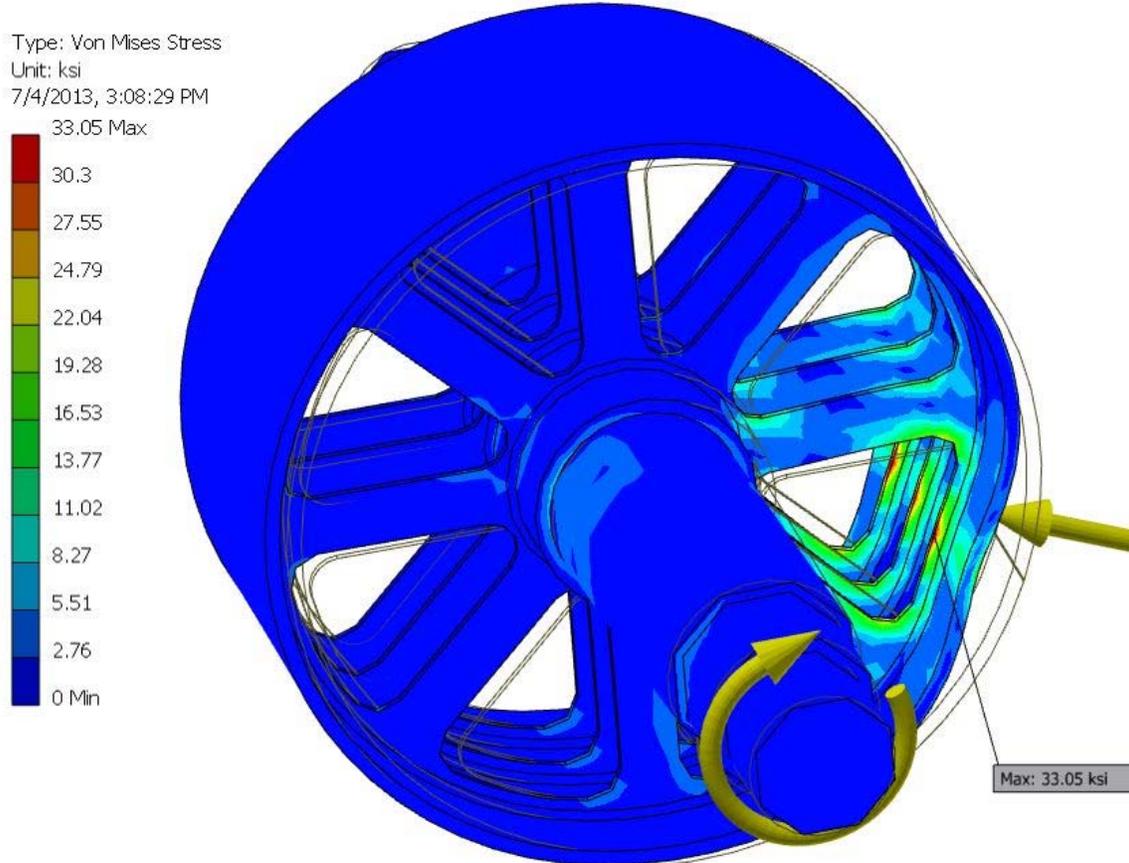
Figure 17.   **Plot of Von Mises stress for a wheel spinning at 2,400 RPM with the compressive load of 3,333 lbs applied . The maximum dynamic stress is 33.05 ksi on the rim at the point of contact. Because of limitations in the finite element software, these analyses neglect some forces and stresses that need to be evaluated. The Hertzian contact stress[8,9] at the point of contact is not accurately modeled here because the mesh is too coarse and the concentrated load does not model the true nature of contact between wheels.   Tractive stress is also not considered here.   During the acceleration of the wheels there are additional inertial terms that increase the stress. All of these factors must be included to verify that the wheel is safe to rotate at its maximum speed (and are not covered here.)**

International Space Elevator Consortium
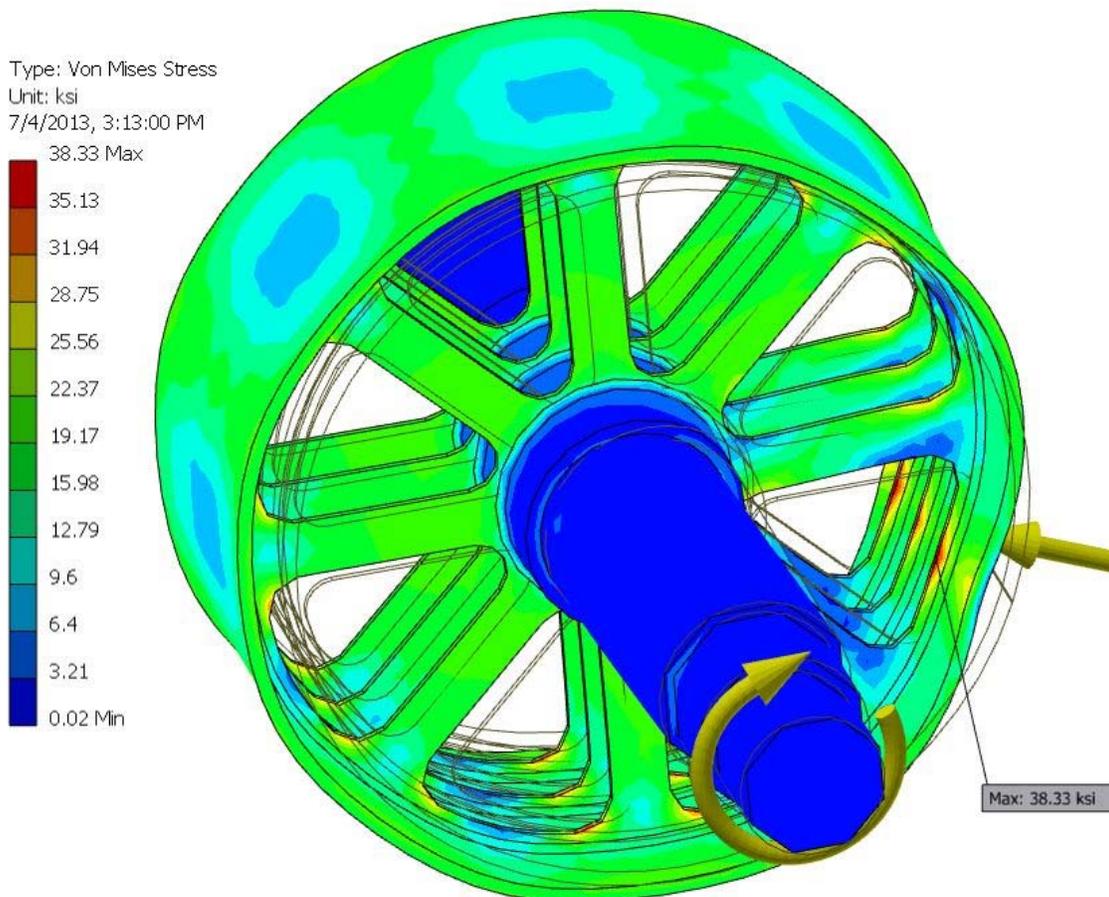
Figure 18. **Plot of Von Mises stress for a wheel spinning at 10,000 RPM with the compressive load of 3,333 lbs applied . The maximum dynamic stress is 38.33 ksi on the rim at the point of contact.**

A much more careful analysis has to be done to verify that a wheel can be as large as 12.8 inches in diameter and rotate at 10,000 RPM. This analysis shows the tight interrelationship between wheel size, motor torque, friction of the ribbon and the speed of the climber. More different designs and materials will also need to be considered to minimize the mass of the wheels and axles. This analysis was purely static stress and used the simplest modifications to the original CAD model. This kind of finite element analysis does not address the possibility of buckling the spokes of the wheel from compressive stress. That is an additional necessary analysis not begun here.

If the rotational velocity of the motor and wheel can be increased to 10,000 RPM, the speed of the climber with 12.8" diameter wheels will be 610.7 km/hr, well over anything considered so far.

One complication of running the climber at higher speed at higher altitude on the ribbon is that the ribbon splicing mechanism (which is the whole purpose of the construction climbers,) would have to be able to handle the increased speed. The implications for this mechanism are beyond the scope of this paper.

In summary, the original combination of an aluminum axle and a titanium wheel weighed 31.0 lbs. The new lighter design weighs 21.9 lbs. This is a reduction of 29.4% on components that represented only 13.11% of the weight of the traction drive system. As mentioned before, much more work has to be done to drastically reduce the mass of the compression mechanism and its structure.

V.   The Problem of the Axial Gap Motors

Edwards and Westling proposed that the most efficient motor for the climber is an axial gap electric motor. Qualitatively, the difference between a conventional radial gap motor and an axial gap motor is that conventional motors are smaller in diameter than they are long. The magnetic field that rotates the rotor is radial. An axial gap motor is short along its output shaft axis and large in diameter. The magnetic field is axially oriented. Axial gap

International Space Elevator Consortium

motors are very common in devices such as the disk drives of computers. They are very efficient and compact, however, as Equations 13 and 14 show, because they are larger in diameter than radial gap motors, the stress in the rotor will be higher for a given rotational speed than it would be in a radial gap motor. Stress increases as a squared function of the radius of the motor. Motors in the 20kW range and up have been designed and built, but have yet to see widespread commercialization. I have found a source for motors up to 100kW for hybrid and electric vehicle use from NuGen Mobility, Inc. Examples of how the real motor parameters effect the climber design are shown above in section IV.

When I began the conceptual design of the climber back in 2004, I contacted Rick Halstead of Empire Magnetics, Inc as that company is known for motors that are designed for severe environments such as vacuum and radiation. At the time, Rick was very interested in developing axial gap motors and gave me information about his conceptual design of 20 and 50 kW motors. Electric cars are an ideal market for motors in that power range.

I contacted Rick in March of 2013 in preparation for this paper and the outlook on the commercialization of large axial gap motors looked bleak. In Rick's words, the "Great Recession" of 2008 caused "everybody to retrench as opposed to expanding. In addition, the fact that the Chinese forced the price of rare earth magnets up over 700% (they have fallen back so now its only about 350%) put a real damper on axial gap developments as they are magnet intensive."

I found information on the web about a motor designed using an SBIR grant by Launchpoint Technologies. This motor is for aerospace use and has dual Hallback arrays of magnets in the rotor and stator. It is claimed to be the highest power density motor available, but it has only been prototyped in a 6 inch diameter. The concept looks very promising.

As I pointed out in 2004, the motors for the space elevator will be custom designed for the many different harsh environments they will see and that design process and prototyping will be expensive. Without knowing the torque-speed curve for the motors, it is impossible to fully characterize the acceleration of the climber or calculate precisely how long the trip to the end of the ribbon will take.

Figure 19 uses all of the motor data I've been able to collect on the mass of the motor as a function of motor power. It is obvious from the chart that there is a very wide spread in the estimates of motor mass. The blue data from NuGen Mobility, Inc is actual motor data, not estimates. Unfortunately, it also represents the heaviest motors for the power. Eric Takamura of NuGen pointed out to me that there is a poor correlation between motor mass and power because there are so many variables that effect the power of a motor. The two points of the same mass on the blue curve at 7.5 and 9.5 kW are caused by changing the voltage of the motor controller from 48V to 72V.
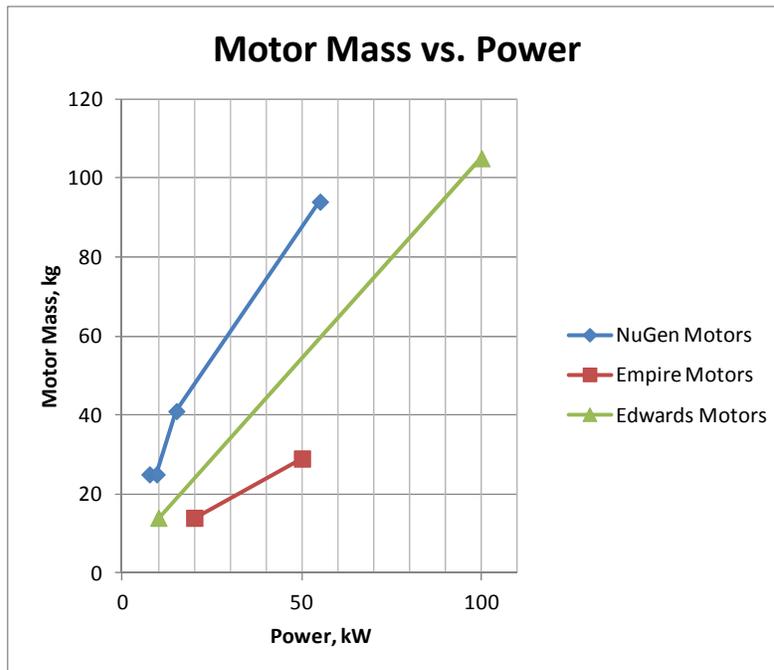
Figure 19. Graph of motor mass as a function of power from several different sources.

NuGen also has a controller technology developed for solar car motors that could be very useful to the Space Elevator given the dramatic differences in the power and torque required as a function of altitude. They have developed a controller that can change the effective ratio between the torque and the output speed of their motors. This means that the same physical motor can have very different torque/speed curves. The controller can decrease the torque by up to a factor of 2.7 and increase the speed of the motor by 2.7. At low altitude, the motor can be run in a lower speed higher torque regime, and then as the gravitational drag drops off the motor can accelerate to a higher speed, lower torque and make up the time lost at low altitude.

The green line in the graph comes from the motor powers and masses quoted in reference 1. I do not know where Edwards and Westling got their estimated motor data from.

The red line in the graph is information provided to me in 2004 by Rick Halstead of Empire Magnetics. It is possible that the mass estimate shown did not include every feature of a real motor, but was based on the major components like the conductors and magnets.

Both NuGen Mobility and the Launchpoint website discuss some of the variations that can be done to minimize the mass of a motor, such as replacing the structural parts with carbon composites.

It is clear at this point that we do not know the mass of the motors that need to be custom designed specifically for the Space Elevator, so it is not possible to know right now if they satisfy the mass budget of the first climber. From discussion with Eric of NuGen, it is also clear that the motors shown in the 2004 conceptual model are roughly the right overall size for the power needed. The mass reduction will come from changing materials, not changing size. I am encouraged by some of the ideas I found for controller technology and motor construction materials that it is still within the realm of possibility to satisfy the mass budget.

VI. The Climber and the Safety Factor of the Ribbon

In 2004, Eric Westling was kind enough to provide the spreadsheet that sized the initial ribbon. Figure 20 shows a screen shot of the spreadsheet. The equations to analytically calculate the cross-section of the ribbon are very complex and difficult to solve, but the problem is amenable to finite difference methods using a spreadsheet to break the ribbon into segments. The spreadsheet breaks the ribbon into 100 km long segments and calculates the tension in the segment starting at the Earth's surface with the climber hanging motionless on the ribbon. The force from the weight of the 900 kg climber is applied at the bottom edge of the first segment, putting it into tension. The force applied at the bottom edge of the next segment up is the tension in the previous segment plus the mass of the previous segment multiplied by the average acceleration due to gravity between the top and bottom of the previous segment. The averaging of g is necessary as g decreases up the height of the ribbon.

Once the row has calculated the value for g at a given altitude and the tension force in the segment, the spreadsheet uses a safety factor of 2 on the tensile strength of the ribbon (130 GPa) to calculate the cross-sectional area of ribbon necessary to carry the tension. The spreadsheet then calculates the mass of the ribbon up to the given altitude by calculating the volume of the ribbon segment (cross-sectional area times length of segment,) multiplied by the density of carbon nanotubes (1300 kg/m^3,) multiplied by the average acceleration due to gravity and adding that to the mass calculated in the cell above. The acceleration due to gravity is the g(r) term defined for Equation 1 above and containing the correction for the rotation of the Earth.

The next two columns of the spreadsheet are used to calculate the total launched mass and the weight of the counterweight needed at the end of the ribbon.

The spreadsheet was constructed to allow a space elevator to be designed for many planets and moons in our Solar System. The information about the other bodies besides the Earth was hidden before taking the screen shot to reduce the clutter in the image.

It is very difficult to calculate anything analytically about the space elevator because everything changes as a function of altitude. The force of gravity is decreasing as $1/r^2$, but the centrepital force increases with r, eventually overtaking gravity and causing the climber to be thrown away from Earth above geosynchronous orbit. The cross-sectional area of the ribbon is minimum at the surface of the Earth, grows to its maximum area at GEO, then decreases again out to the end of the ribbon. The spreadsheet does all these things in a very clever way with only small errors coming from the segment size.

Because all of these things are changing continuously, it is important to remember that everything is local on the space elevator. The mass of the counterweight is only that which is needed to balance the tension in the ribbon immediately below it.

The only problem I see with the way the elevator is sized in the spreadsheet is that there is no allowance for the acceleration of the climber. The effective weight of the climber is its gravitational weight plus its inertial weight from acceleration. If the climber were to suddenly accelerate upward at one gee, the climber would effectively

weigh twice as much to the ribbon and the safety factor would be consumed. In designing the Space Elevator for real, I would modify the first term in the spreadsheet to include both the weight of the climber and its maximum acceleration near the surface of the Earth. This will cause the pilot ribbon to be a little more massive (higher tension leads to larger cross-sectional area of CNTs,) but slightly more conservative in design. Since the Space Shuttle has been decommissioned, the payload of the Shuttle is no longer a factor in the design of the pilot ribbon. Some other rocket will be necessary to boost the first ribbon to Low Earth Orbit (LEO). Given this fact, I would also eliminate the double spool described in the book and boost a single pilot ribbon to LEO.

	A	B	C	D	E	F	G	H
1			CNT density, kg/m^3	planet radius, m	Step size	tensile, Pa	lift (kg)	G
2			1300	6378000	0.01568	1.30E+11	900	6.67E-11
3				Safety Factor			519.2578669	PL
4				2			380.7421331	CW
5			MG/r-rw2					
6		Select	Planet	Mass, kg	Diameter, km	period (day)	ang vel, rad/sec	step
8		1	Earth	5.98E+24	12756	1	7.29212E-05	0.015678896
24			selected values	5.98E+24	12756		7.3E-05	0.01568
25								
26		106378	31.00	4.77E-10	35.53147464			
27		step size, m	3.4E-02	0.062004148	cm wide	22043.9275	38207.48039	16163.5529
28		100000	9.772293124		13.53	40079.9	69468.1	29388.3
29	Altitude, km	radius, m	g accel, m/s^2	tension, N	cable cross A, m^2	Integrated Cable mass, kg	Total launched mass, kg	Counterweight mass, kg
30	0	6378000	9.77E+00	8.80E+03	1.35E-07	0.00		0.73
31	100	6478000	9.47E+00	8.96E+03	1.38E-07	17.59	CW/ratio	
32	200	6578000	9.18E+00	9.13E+03	1.40E-07	35.52		
33	300	6678000	8.91E+00	9.30E+03	1.43E-07	53.78		
34	400	6778000	8.65E+00	9.46E+03	1.46E-07	72.38		
35	500	6878000	8.40E+00	9.62E+03	1.48E-07	91.30		

Figure 20. Screen shot of the Excel spreadsheet that sized the pilot ribbon of the Space Elevator.

VII. General Comments on Climber Design

Figure 21.   Model climber on the tether with the center of mass off to one side of the ribbon. The climber is distorting the ribbon to put the center of mass directly under it.

In thinking about the climber suspended from the ribbon it helps to think about the way heavy objects are rigged from cranes. The key fact of any rigging job is that the center of gravity (C.G.) of the load will always be directly below the lifting point. The crane hook and the cable cannot support a bending moment, so the load will just rotate downward until the C.G. is directly below the hook and there is no moment.

This fact was obvious in one of the photos of the toy climber competition at the 2011 Space Elevator Conference. Figure 21 shows what happens to the ribbon when the climber's center of mass is not centered on the ribbon. The ribbon cannot support a bending moment, so the ribbon must be deformed until there is a balance of forces between the tension in the ribbon and the moment caused by the offset C.G.

Another important point to keep in mind is that besides being centered on the ribbon, the center of mass must also be below the traction drive. If a climber is loaded above the traction drive, even if the C.G. is centered, it is metastable. Any perturbation of the climber will cause the climber to try to capsize until the C.G. is below the traction drive.

This raises the interesting question about what happens to a climber above GEO. Effectively, above GEO the climber is upside down if its center of mass is closer to the Earth than the traction drive. It is in a metastable configuration. It is not clear to me whether the centrepital acceleration above GEO is low enough that it cannot capsize

22

the climber against the tension in the ribbon.

One possible way to avoid that instability is if the climber is capable of reconfiguring itself above GEO. If the payload were on a linear bearing track that allowed it to take positions above or below the traction drive, it could switch positions above GEO. The details of this would depend on the payload. Any linear bearing system would reduce the available mass for the payload.

VIII. Conclusion

It was not possible to definitively determine whether the 2004 conceptual design of the first climber can be lightened enough to satisfy the mass budget in Edwards' and Westling's book. Further work has shown that there is a narrow range to the practical diameter of the wheels on the climber. Wheels that are too small would have to spin too fast and too many times to lift the climber at useful speed. Wheels that are too large cause the braking torque of the climber to be too high for practical motors and their dynamic stress becomes too large for real materials.

The climber will need more power than previously estimated to climb at useful speeds. It will require clever and detailed engineering to design motors in the appropriate power range that are light enough to satisfy the mass budget. Right now nothing certain can be said about the mass of a 100 kW motor for the Space Elevator.

Fatigue of the rolling elements of the climber must be in the mind of the designer at all times. The 100,000 km long ribbon requires the climbers to live most of the life of an Earth electric car within one month and one trip with no repair stations.

The structure around the compression drives of the floating axle modules in the 2004 design is where the bulk of the structural material is and where the greatest effort is needed in redesign to lower this mass.

The drag force of gravity pulling the climber down the ribbon drops off very quickly with altitude up the ribbon. Given the very large power and torque capability necessary near the surface of the Earth, the climbers may be able to accelerate well past 200 km/hr at the higher altitudes, as long as the fatigue strength of the rolling components is not exceeded. The trip to the end of the ribbon will not be at either constant velocity or constant power, but the best mix of power and speed to make the total trip length practical.

Acknowledgments

References

[1]Bartoszek, L. 2004. "A Preliminary Ribbon Climber Mechanical Design With Focus on Tribology and Fatigue", 3rd International Space Elevator Conference, 6/28-30/04, Washington, DC

[2]Edwards, B. and Westling, E. (2003) *The Space Elevator—a revolutionary Earth-to-space transportation system*, BC Edwards, Houston.

[3]Bathias, C. and Paris, P. (2005) *Gigacycle Fatigue in Mechanical Practice*, Marcel Dekker, NY

[4] http://www.ngmcorp.com/index.htm

[5]Lampman, S. (1996) *ASM Handbook Volume 19 Fatigue and Fracture*, ASM International, Ohio

[6]Boyer, H. (1986) *Atlas of Fatigue Curves*, ASM International, Ohio

[7]Shigley, J. and Mischke, C. (1989) *Mechanical Engineering Design*, McGraw-Hill, New York.

[8]Johnson, K. (1985) *Contact Mechanics*, Cambridge University Press, Cambridge.

[9]Shigley, J. and Mischke, C. (1986) *Standard Handbook of Machine Design*, McGraw-Hill, New York.